LETTERS

Gulf Stream density structure and transport during the past millennium

David C. Lund[1]†, Jean Lynch-Stieglitz[2] & William B. Curry[3]

The Gulf Stream transports approximately 31 Sv (1 Sv = 10^6 m^3 s^{-1}) of water[1,2] and 1.3 × 10^{15} W of heat[3] into the North Atlantic ocean. The possibility of abrupt changes in Gulf Stream heat transport is one of the key uncertainties in predictions of climate change for the coming centuries. Given the limited length of the instrumental record, our knowledge of Gulf Stream behaviour on long timescales must rely heavily on information from geologic archives. Here we use foraminifera from a suite of high-resolution sediment cores in the Florida Straits to show that the cross-current density gradient and vertical current shear of the Gulf Stream were systematically lower during the Little Ice Age (AD ~1200 to 1850). We also estimate that Little Ice Age volume transport was ten per cent weaker than today's. The timing of reduced flow is consistent with temperature minima in several palaeoclimate records[4–9], implying that diminished oceanic heat transport may have contributed to Little Ice Age cooling in the North Atlantic. The interval of low flow also coincides with anomalously high Gulf Stream surface salinity[10], suggesting a tight linkage between the Atlantic Ocean circulation and hydrologic cycle during the past millennium.

The Florida Current, the portion of the Gulf Stream that flows through the Straits of Florida, is characterized by a strong cross-current gradient in seawater density. This gradient reflects a flow that is in approximate geostrophic and hydrostatic balance, and it is proportional to the vertical shear in current velocity. Past changes in current shear can be estimated using two vertical profiles of seawater density, one from each side of the Florida Current. To reconstruct density profiles for the past millennium, we used foraminifera from sediment cores retrieved near Dry Tortugas and Great Bahama Bank (Fig. 1). The $\delta^{18}O$ of foraminifera ($\delta^{18}O_c$) depends on the temperature and the $\delta^{18}O$ of sea water ($\delta^{18}O_w$) in which they live. Because $\delta^{18}O_w$ is linearly related to salinity, and the difference between $\delta^{18}O_w$ and $\delta^{18}O_c$ is thermodynamically controlled, seawater density can be estimated using $\delta^{18}O_c$ (ref. 11; see Methods).

To estimate volume transport using the geostrophic technique, a reference velocity must be known or estimated to provide a constant of integration for the vertical shear profile. Typically, a level of no motion is assumed near the bottom of the flow. Today, near-zero velocities in this part of the Florida Straits occur below 800 m (refs 2, 12). We used a level of no motion at a water depth of 850 m, which yields a modern transport of 31 Sv (see Methods and Supplementary Information on transport calculation). This value is consistent with flow estimates obtained using current meter[13–15], geostrophic[16], cable voltage[1,17], dropsonde[14,18], and Pegasus acoustic profiler techniques[2].

The Florida Current density time series are based on over 3,000 stable isotopic measurements of foraminifera calcifying at water depths ranging from the surface to 750 m and ranging in age from ~0 to 1,100 yr ago (Fig. 2). Planktonic foraminiferal $\delta^{18}O_c$ was used to constrain the density of the surface mixed layer. The annual average mixed layer in this region is approximately 50 m (ref. 19), similar to the depth habitat of *Globigerinoides ruber*[20,21]. Near Dry Tortugas, planktonic $\delta^{18}O_c$ was constant (within 95% confidence limits) from 2,000 to 900 yr before present (BP), but then increased by 0.3‰ ($\Delta\sigma_t$ = ~0.5) from 900 to 400 yr BP, with the largest shift after 600 yr BP (Fig. 2a). On the Bahamas side of the Florida Straits, $\delta^{18}O_c$ was stable from 2,000 to 250 yr BP, and then increased 0.2‰ ($\Delta\sigma_t$ = ~0.3) from 250 yr BP to present (Fig. 2b). Surface water $\delta^{18}O_c$ variability at each site was driven primarily by changes in $\delta^{18}O_w$ (ref. 10).

The benthic $\delta^{18}O_c$ records show that changes in Florida Current density structure occurred during the past millennium (Fig. 2c, d). From ~1,100 to 900 yr BP, $\delta^{18}O_c$ increased by 0.1‰ ($\Delta\sigma_t$ = ~0.1) along the Great Bahama Bank, yet there was little change at the Dry Tortugas sites, yielding a decrease in cross-current density gradient and vertical current shear. A further reduction in shear occurred from 900 to 200 yr BP, because $\delta^{18}O_c$ decreased by 0.1‰ at intermediate water depths near Dry Tortugas, while remaining nearly constant along the Great Bahama Bank. From 200 yr BP to the present, benthic $\delta^{18}O_c$ at all the Bahamas sites decreased by 0.1‰ ($\Delta\sigma_t$ = ~0.1), with no comparable change at Dry Tortugas. This density gradient increase reflects enhanced vertical shear in the Florida Current during the past 200 yr.

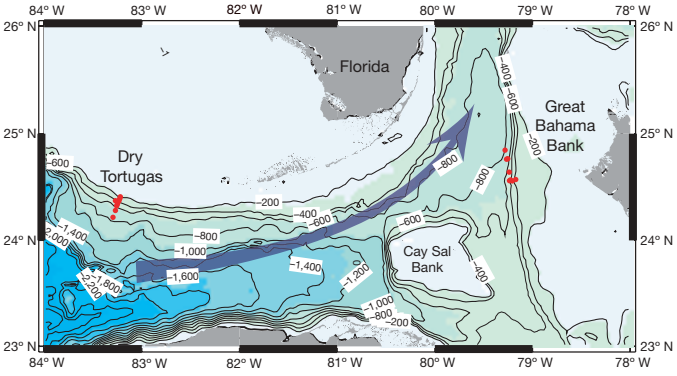

Figure 1 | Bathymetric map of Florida Straits showing core locations (red circles). Near Dry Tortugas, we used seven cores at five separate water depths, spanning 200 to 750 m (Supplementary Table 1). On the Great Bahama Bank, a total of seven cores were used at four water depths from 260 to 700 m (Supplementary Table 2). Contours indicate water depth in metres. All cores reported here, except W167-79GGC (ref. 30), were collected in January 2002 aboard the R/V *Knorr*. Approximately 28 Sv of transport occurs between Cay Sal Bank and Florida (blue arrow)[2,16,17], while ~2 Sv flows through the Santaren channel between Cay Sal Bank and Great Bahama Bank[2].

[1]Massachusetts Institute of Technology/Woods Hole Oceanographic Institution Joint Program in Oceanography, Woods Hole, Massachusetts 02543, USA. [2]School of Earth and Atmospheric Sciences, Georgia Institute of Technology, Atlanta, Georgia 30332, USA. [3]Department of Geology and Geophysics, Woods Hole Oceanographic Institution, Woods Hole, Massachusetts 02543, USA. †Present address: Division of Geological and Planetary Sciences, California Institute of Technology, Pasadena, California 91125, USA.

Using the foraminifera-based seawater density data from Fig. 2, we estimate that Florida Current volume transport varied by 3±1 Sv during the past millennium, or about 10% of the total flow (Fig. 3b). Compared to the 10–15 Sv estimated flow reduction for the Last Glacial Maximum[22], the Florida Current is characterized by modest variations in volume transport during the latest Holocene. However, there is a distinct interval of low flow from ~700 to 100 yr BP—the approximate time of maximum cooling in several North Atlantic temperature records[4–9]. The similar timing of changes in North Atlantic temperature and Florida Current strength suggests that reduced northward oceanic heat transport may have contributed to cooler temperatures during the Little Ice Age. Heat flux is a function of both volume transport and the temperature difference between the Florida Current and water flowing southward out of the North Atlantic[3], so temperature reconstructions from these flows will be necessary to confirm past changes in oceanic heat transport.

In addition to total volume transport, the $\delta^{18}O_c$-based density records yield information on the variability in transport with depth. The Florida Current consists of two primary components, one from the South Atlantic that is fresh (salinity < 36) and the other from the North Atlantic subtropical gyre that is salty (salinity > 36). The fresh component is found at the surface (>24 °C) and bottom (7–12 °C) of the Florida Current, accounts for ~14 Sv of the total transport, and acts as the northward-flowing upper limb of the meridional overturning circulation (MOC)[23]. The deepest portion of the Florida Current contains Antarctic Intermediate Water that has been modified through mixing with saltier water of the subtropical gyre. The wind-driven subtropical gyre component sits between the fresh South Atlantic water at the surface and deepest parts of the Florida Current, is characterized by intermediate temperatures (12–24 °C), and accounts for ~17 Sv of the total flow[24].

Reduced transport during the Little Ice Age is a function of lower flow throughout the water column, but the largest negative anomalies occur at depths from 100 to 500 m (or $24 < \sigma_t < 27$) (Fig. 3a). This is the density range associated with waters from the North Atlantic subtropical gyre, so it appears that the wind-driven component of the Florida Current was primarily responsible for low total transport during the Little Ice Age. The intervals 0–100 yr BP and 1,000–1,100 yr BP are characterized by higher transport, but they differ in that the modern anomaly spans the entire water column, whereas at 1,100 yr BP it is concentrated above 500 m. This pattern suggests that the flow of upper Antarctic Intermediate Water was weaker at 1,100 yr BP than it is today.

Flow anomalies below 500 m water depth are small for two reasons. First, we assume a level of no motion at 850 m and therefore departures from this reference point are minimized. Second, when contoured in terms of Sverdrups, the anomalies below 500 m appear small because total volume transport in this depth range is low relative to transport above 500 m. If we instead contour the percentage change in flow relative to the long-term mean, we observe a transport

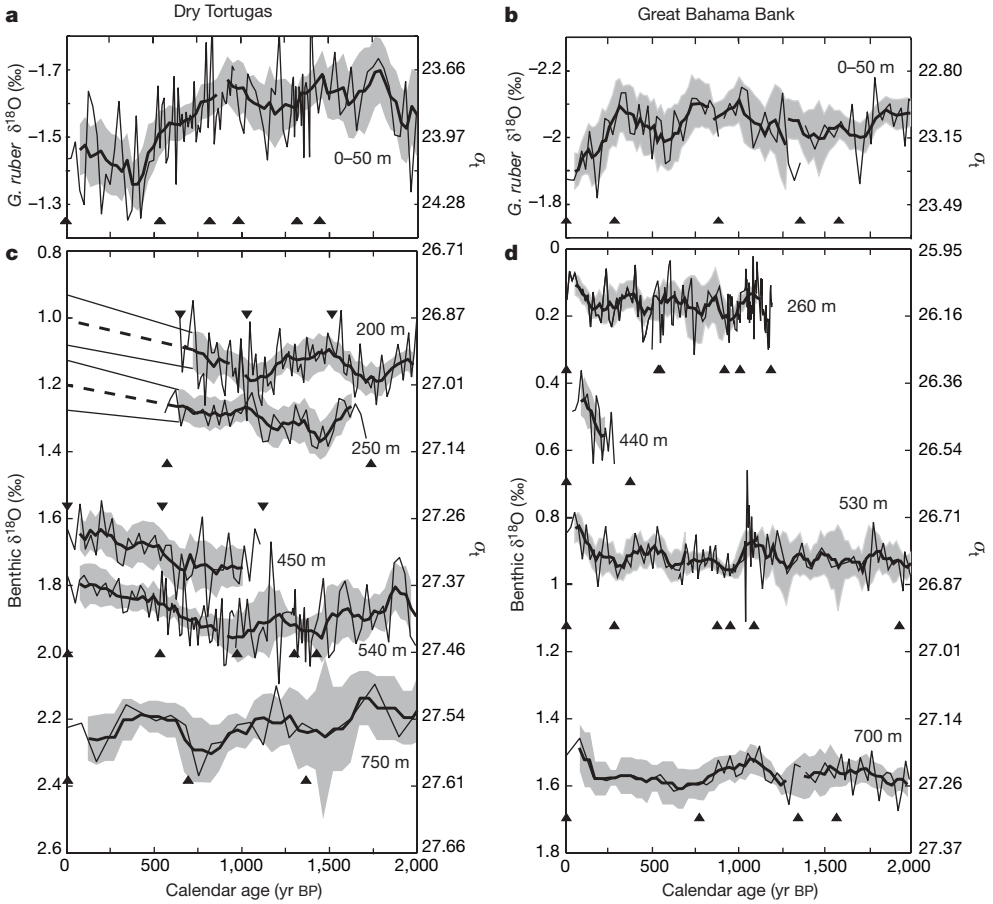

Figure 2 | Foraminiferal $\delta^{18}O_c$ data for Florida Straits cores. Plotted are the average $\delta^{18}O_c$ value at each stratigraphic level (thin black line), the running mean (thick black line), and the 95% confidence limit on the running mean (shaded area) (see Methods). Triangles represent calendar-corrected radiocarbon ages (Supplementary Tables 1 and 2). **a**, *G. ruber* $\delta^{18}O_c$ for Dry Tortugas. **b**, *G. ruber* $\delta^{18}O_c$ for Great Bahama Bank. **c**, Benthic $\delta^{18}O_c$ for Dry Tortugas. To fill the gap between 500 yr BP and today (at 200 and 250 m), we interpolated between σ_t values based on CTDs and core tops (Supplementary Fig. 4). The resulting trend (dashed line) is similar to that in deeper cores, suggesting that it is a reasonable approximation of density for this time interval. The maximum $\delta^{18}O_c$ uncertainty for these sites is ±0.1‰ (±3σ) ($\delta^{18}O_c$ must always be larger at 250 m than at 200 m), equivalent to a 95% confidence limit of ±0.07‰. Uncertainty between today and 500 yr BP was estimated by interpolation between the ±0.07‰ envelope and core top uncertainties. **d**, Benthic $\delta^{18}O_c$ for Great Bahama Bank. The time series at 440 m was not used in the transport calculation because it is too short, but the trend of decreasing $\delta^{18}O_c$ over the past 200 yr is consistent with the other benthic records from the Bahamas.

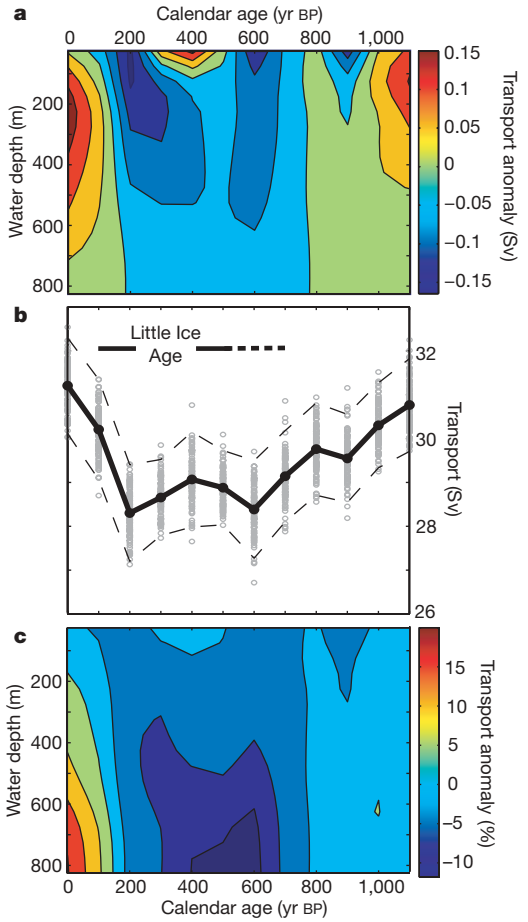

Figure 3 | Transport reconstruction for the Florida Current. a, Flow anomaly versus depth, defined as transport at a given time minus average transport over the period 0–1100 yr BP. Negative transport anomalies occur during the Little Ice Age and are largest in the depth range occupied by water from the North Atlantic subtropical gyre. **b**, Estimated total transport 0–1100 yr BP. The most probable transport values (thick black line) are based on mean densities in Fig. 2. The grey circles represent transport estimates based on density values randomly sampled from within the error envelopes in Fig. 2, while the dashed lines represent the 95% confidence limit for the transport calculation (see Methods). **c**, Flow anomaly versus depth, defined as the percentage change in transport relative to the mean value at a given depth from 0–1000 yr BP. The largest changes occur near the bottom of the Florida Current, the depth range associated with Antarctic Intermediate Water.

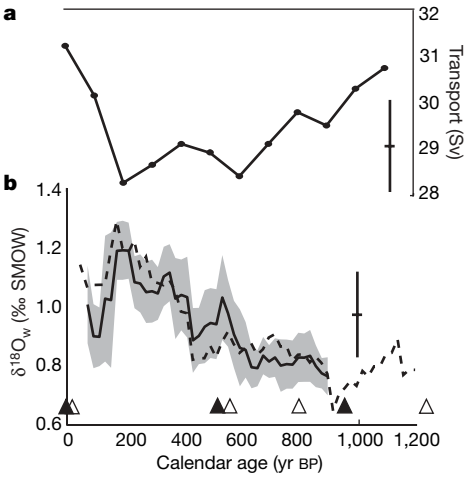

Figure 4 | Comparison of Florida Current transport and surface water $\delta^{18}O_w$ reconstructions. a, Transport 0–1100 yr BP. The vertical bar represents the average 95% error envelope from Fig. 3 (±1 Sv). **b**, Surface water $\delta^{18}O_w$ estimates based on $\delta^{18}O_c$ and Mg/Ca analyses of planktonic foraminifera (*G. ruber*) in two Dry Tortugas cores[10]. Lines represent 100-yr running mean values for $\delta^{18}O_w$ (solid line, KNR166-2-62MC; dashed line, W167-79GGC). The shaded area represents the 95% confidence limit for 62MC. For clarity, the average 95% confidence limit for 79GGC (±0.15‰) is given as a vertical bar. The $\delta^{18}O_w$ error estimates are based on the combined uncertainty of Mg/Ca and $\delta^{18}O_c$ analyses[10]. Symbols indicate calendar-calibrated radiocarbon control points (solid triangles, KNR166-2-62MC; open triangles, W167-79GGC).

reduction of 15–25% during the Little Ice Age relative to today below 500 m water depth (Fig. 3c). This suggests the MOC also played a role in the Little Ice Age transport anomaly. Using only data from the Straits of Florida, it is not possible to quantify the relative contributions of the wind-driven gyre and MOC to the flow variability of the past millennium. Estimating changes in these components will require transport reconstructions from additional sites in the Atlantic.

Although the Little Ice Age is best-known as a time of cooler temperatures and alpine glacier advances in the Northern Hemisphere, it was also characterized by anomalously dry conditions in Central and South America[25,26] and high surface salinity in the Florida Current (Fig. 4). A comparison of Florida Current surface $\delta^{18}O_w$ to the Cariaco Basin aridity record implies that there is a strong climatic link between the two[10]. As originally suggested by ref. 25, the drier conditions probably reflect a southward shift of the Atlantic Inter-Tropical Convergence Zone (ITCZ). On interannual to decadal timescales, small (<1 °C) shifts in the cross-equatorial Atlantic sea surface temperature (SST) gradient can cause the mean ITCZ position to shift more than 1,000 km (ref. 27). We speculate that reduced northward oceanic heat transport during the Little Ice Age altered the tropical Atlantic SST field and triggered southward movement of the ITCZ. This scenario is consistent with evidence for reduced volume transport and high surface salinities in the Straits of Florida (Fig. 4).

Control simulations of the HadCM3 coupled ocean–atmosphere model yield a centennial-scale climate oscillation involving the MOC and the ITCZ[28]. A reduction in the MOC of 2 Sv produces a ~0.1 °C cross-equatorial Atlantic SST contrast that forces southward ITCZ migration and yields positive salinity anomalies in the tropical North Atlantic. The simulated anomalies advect to the high-latitude North Atlantic via the Gulf Stream, and act to enhance the MOC by increasing surface ocean density. The resulting increase in northward oceanic heat transport alters the cross-equatorial Atlantic SST gradient, causing the ITCZ to migrate northwards, producing a negative salinity anomaly in the tropical North Atlantic. As this low-salinity water advects to deep-water convection sites in the Greenland and Nordic Seas, the strength of the MOC diminishes, thus completing the oscillation.

We speculate that a similar coupling occurred during the past millennium, where changes in Gulf Stream salinity acted as a negative feedback on volume transport by modulating the strength of the MOC through buoyancy forcing in the high-latitude Atlantic. It is also possible that southward ITCZ migration, perhaps triggered by low solar irradiance[10], reduced windstress curl over the North Atlantic subtropical gyre and therefore northward oceanic heat transport. In either case, it appears that the Gulf Stream played a key role in the Little Ice Age, perhaps as a feedback in an oscillation internal to the climate system or as an amplifier of externally forced variability.

METHODS

Age control. Age control is provided by multiple radiocarbon dates on planktonic foraminifera in each core (see Supplementary Tables 1 and 2). All raw radiocarbon ages were converted to calendar ages assuming a surface ocean reservoir age of 400 yr (see Supplementary Information on age control). Age models were created by linear interpolation between ^{14}C control points. Average

sedimentation rates for the Dry Tortugas cores range from 11 to 66 cm kyr^{-1}. For the Great Bahama Bank, average sedimentation rates are higher, ranging from 20 to 350 cm kyr^{-1}.

$\delta^{18}O_c$ analyses. Stable isotope analyses for the Florida Straits cores were based on *Cibicidoides* and *Planulina* species. These species follow the fractionation for inorganic calcite precipitation determined in ref. 29, such that the $\delta^{18}O_{calcite} - \delta^{18}O_{seawater}$ difference follows a thermodynamic slope of $\sim$0.2‰ °C^{-1} (see Supplementary Information on sampling strategy). Stable-isotope analyses were performed on a Finnigan MAT 253 coupled to a Kiel III carbonate device. Calibration to the Vienna Pee-Dee Belemnite (VPDB) scale was made using NBS-19 ($\delta^{18}O = -2.20$‰ and $\delta^{13}C = 1.95$‰). Long-term reproducibility (1σ) of NBS-19 ($n = 461$) for this mass spectrometer system is $\pm$0.08‰ for $\delta^{18}O$ and $\pm$0.04‰ for $\delta^{13}C$.

The 95% confidence limits for the running-mean $\delta^{18}O_c$ values in Fig. 2 are based on the Student's *t*-distribution (upper limit = $M + t(\sigma/\sqrt{n})$; lower limit = $M - t(\sigma/\sqrt{n})$; where M is the running mean, t is the two-tailed *t*-value, σ is the standard deviation of $\delta^{18}O_c$ analyses for a given time window, and n is the number of analyses). The length of the smoothing window for each core was chosen such that each running-mean $\delta^{18}O_c$ value is based on an average 15–25 individual $\delta^{18}O_c$ analyses (for $\alpha = 0.05$ and $n = 20$, $t = 2.09$). All of the Dry Tortugas cores were smoothed using a 150-yr window, except the lowest-sedimentation-rate core (at 750 m water depth), where we used a 250-yr window. The Great Bahama Bank $\delta^{18}O_c$ time series were smoothed with a 100-yr window, except at 700 m water depth, where a 150-yr window was used.

Density calibration. We quantified the relationship between foraminiferal $\delta^{18}O$ ($\delta^{18}O_c$) and seawater σ_t by: (1) estimating seawater $\delta^{18}O$ ($\delta^{18}O_w$) for conductivity–temperature–depth (CTD) data taken at the core sites using the $\delta^{18}O_w$–S relationship from North Atlantic thermocline waters; (2) calculating the predicted $\delta^{18}O_c$ of foraminifera precipitated in equilibrium with this water; (3) determining σ_t values for the CTD data, and finally (4) creating a regression between σ_t and $\delta^{18}O_c$ (see Supplementary Information on density calibration). The resulting polynomial fit was used to estimate past changes in seawater density. Density values based on foraminifera from the most recent (core top) sediment in each core are very similar to density values determined using temperature and salinity data from CTD casts (see Supplementary Fig. 4).

Transport calculation. Transport estimates were made using the thermosteric anomaly, which is the primary component of specific volume anomaly in the upper 1,000 m of the ocean and can be calculated directly from σ_t (see Supplementary Information on transport calculation). We used a level of no motion (850 m) that yields a core top transport of 31 Sv, similar to the modern instrumental value. This level of no motion is consistent with current meter data that show near-zero velocities between Cay Sal Bank and Florida at 800–1,000 m (ref. 2). Offshore of Key West, the level of no motion is deeper ($\sim$1,000 m) but all velocities below 600 m are less than 5 cm s^{-1} (ref. 12). In the much shallower Santaren Channel, near-zero flow velocities occur near 600 m (ref. 2). A level of no motion at 900 m yields a transport of 33 Sv, which is higher than published values of annual average flow for the Florida Current at this location.

We estimated uncertainty in the transport calculation using a Monte Carlo approach. For each time interval, transport was calculated using σ_t values randomly sampled from the observed probability distribution in each core (Fig. 2), which reflects the analytical and sampling uncertainty of the $\delta^{18}O_c$ analyses. We repeated this process 100 times at each 100-yr increment from 0 to 1,100 yr BP (Fig. 3; grey circles). The 95% error envelope (Fig. 3; dashed lines), defined here as $\pm 2\sigma$ of the Monte Carlo estimates, averages $\pm$1 Sv. Reasonable changes in the $\delta^{18}O_w$–S relationship have a small ($<$0.5 Sv) impact on transport (see Supplementary Information on $\delta^{18}O_w$–S transport error).

Received 14 March; accepted 19 September 2006.

1. Baringer, M. O. & Larsen, J. C. Sixteen years of Florida Current transport at 27°N. *Geophys. Res. Lett.* **28,** 3179–3182 (2001).
2. Leaman, K. D. *et al.* Transport, potential vorticity, and current/temperature structure across Northwest Providence and Santaren Channels and the Florida Current off Cay Sal Bank. *J. Geophys. Res.* **100** (C5), 8561–8569 (1995).
3. Larsen, J. C. Transport and heat flux of the Florida Current at 27°N derived from cross-stream voltages and profiling data: theory and observations. *Phil. Trans. R. Soc. Lond. A* **338,** 169–236 (1992).
4. Lamb, H. *Climate, History and the Modern World* edn 2 (Routledge, London/New York, 1995).
5. Keigwin, L. D. The Little Ice age and Medieval Warm Period in the Sargasso Sea. *Science* **274,** 1504–1508 (1996).
6. Dahl-Jensen, D. *et al.* Past temperatures directly from the Greenland ice sheet. *Science* **282,** 268–271 (1998).
7. deMenocal, P., Ortiz, J., Guilderson, T. & Sarnthein, M. Coherent high- and low-latitude climate variability during the Holocene warm period. *Science* **288,** 2198–2202 (2000).
8. Marchitto, T. M. & deMenocal, P. B. Late Holocene variability of upper North Atlantic Deep Water temperature and salinity. *Geochem. Geophys. Geosyst.* **4,** 1100, doi:10.1029/2003GC000598 (2003).
9. Esper, J., Cook, E. R. & Shweingruber, F. H. Low-frequency signals in long tree-ring chronologies for reconstructing past temperature variability. *Science* **295,** 2250–2253 (2002).
10. Lund, D. C. & Curry, W. B. Florida Current surface temperature and salinity variability during the last millennium. *Paleoceanography* **21,** PA2009, doi:10.1029/2005PA001218 (2006).
11. Lynch-Stieglitz, J., Curry, W. B. & Slowey, N. A geostrophic estimate for the Florida Current from the oxygen isotope composition of benthic foraminifera. *Paleoceanography* **14,** 360–373 (1999).
12. Hamilton, P., Larsen, J. C., Leaman, K. D., Lee, T. N. & Waddell, E. Transports through the Straits of Florida. *J. Phys. Oceanogr.* **35,** 308–322 (2005).
13. Pillsbury, J. E. The Gulf Stream—A description of the methods employed in the investigation, and the results of the research. In *Report of the Superintendent of the U. S. Coast and Geodetic Survey* 173–184 (U. S. Coast and Geodetic Survey, Washington DC, 1890).
14. Schmitz, W. J. & Richardson, W. S. On the transport of the Florida current. *Deep-Sea Res.* **15,** 679–693 (1968).
15. Schott, F. A., Lee, T. N. & Zantopp, R. Variability and structure of the Florida Current in the period range of days to seasonal. *J. Phys. Oceanogr.* **18,** 1209–1230 (1988).
16. Montgomery, R. B. Transport of the Florida Current off Habana. *J. Mar. Res.* **IV,** 198–220 (1941).
17. Wertheim, G. K. Studies of the electric potential between Key West, Florida, and Havana, Cuba. *Trans. AGU* **35,** 872–882 (1954).
18. Niiler, P. P. & Richardson, W. S. Seasonal variability of the Florida Current. *J. Mar. Res.* **31,** 144–167 (1973).
19. Carton, J. A. & Giese, B. S. SODA version 1.4.2: A reanalysis of ocean climate. *J. Geophys. Res.* (submitted); preprint at ⟨http://www.atmos.umd.edu/~carton/pdfs/carton&giese05.pdf⟩ (2005).
20. Deuser, W. G. Seasonal variations in isotopic composition and deep-water fluxes of the tests of perennially abundant planktonic foraminifera of the Sargasso Sea: results from sediment-trap collections and their paleoceanographic significance. *J. Foraminiferal Res.* **17,** 14–27 (1987).
21. Anand, P., Elderfield, H. & Conte, M. H. Calibration of Mg/Ca thermometry in planktonic foraminifera from a sediment trap time series. *Paleoceanography* **18,** 1050, doi:10.1029/2002PA000846 (2003).
22. Lynch-Stieglitz, J., Curry, W. B. & Slowey, N. Weaker Gulf Stream in the Florida Straits during the Last Glacial Maximum. *Nature* **402,** 644–648 (1999).
23. Schmitz, W. J. & Richardson, P. On the sources of the Florida Current. *Deep-Sea Res.* **38** (suppl.), 379–409 (1991).
24. Schmitz, W. J., Luyten, J. R. & Schmitt, R. W. On the Florida Current T/S envelope. *Bull. Mar. Sci.* **53,** 1048–1065 (1993).
25. Haug, G., Hughen, K. A., Sigman, D. M., Peterson, L. C. & Rohl, U. Southward migration of the Inter-Tropical Convergence Zone through the Holocene. *Science* **293,** 1304–1308 (2001).
26. Hodell, D. A. *et al.* Climate change on the Yucatan Peninsula during the Little Ice Age. *Quat. Res.* **63,** 109–121 (2005).
27. Chiang, J., Kushnir, Y. & Giannini, A. Deconstructing Atlantic Intertropical Convergence Zone variability: Influence of the local cross-equatorial sea surface temperature gradient and remote forcing from the eastern equatorial Pacific. *J. Geophys. Res.* **107,** doi:10.1029/2000JD000307 (2002).
28. Vellinga, M. & Wu, P. Low-latitude freshwater influence on centennial variability of the Atlantic thermohaline circulation. *J. Clim.* **17,** 4498–4511 (2004).
29. Kim, S. & O'Neil, J. Equilibrium and non-equilibrium oxygen isotope effects in synthetic carbonates. *Geochim. Cosmochim. Acta* **61,** 3461–3475 (1997).
30. Lund, D. C. & Curry, W. B. Late Holocene variability in Florida Current surface density: Patterns and possible causes. *Paleoceanography* **19,** PA4001, doi:10.1029/2004PA001008 (2004).

Supplementary Information is linked to the online version of the paper at www.nature.com/nature.

Acknowledgements We thank O. Marchal, L. Keigwin, D. Oppo and J. McManus for suggestions. We also thank D. Ostermann, M. Jeglinski, P. Cerulli, S. Thorrold and S. Birdwhistle for technical support. We are grateful to the WHOI core lab for sample collection and archiving, the captain and crew of the R/V *Knorr*, and to the Sea Education Association for access to their vessel *Westward*. This work was supported by the US National Science Foundation.

Author Information Reprints and permissions information is available at www.nature.com/reprints. The authors declare no competing financial interests. Correspondence and requests for materials should be addressed to D.C.L. (dlund@gps.caltech.edu).